REVIEW PAPER

An Improvedu-Net Model for Carotid Plaque Segmentation

Prathiba Jonnala[1]* and Dr.G. Sitaramanjaneya Reddy[2]

[1,2] *Vignan's Foundation for Science, Technology and Research (Deemed to be University), Vadlamudi, Andhra Pradesh, India*

[1]**jp_ece@vignan.ac.in*

Received: 16th Dec, 2025; Revised: 8th Feb 2026; Accepted: 12th Feb, 2026; Available Online: 28th Feb, 2026

ABSTRACT

Medical imaging has evolved into a standard in diagnosis and treatment for the visual portrayal of organ and tissue functioning. For clinical diagnosis, processing and analysis of these medical images are therefore crucial. According to WHO (World Health Organisation), CVDs (cardiovascular diseases) are major causes for mortalities in people.; DL (deep learning) based image segmentation has attracted a lot of interest over the past several years, which emphasises the need for a thorough analysis of it. Carotid Plaque is not correctly segmented by current U-Net Models. Improved U-Nets are presented for semantic segmentations for precise comprehensions in this study to address the problem. To achieve a more precise detection, the semantic segmentation is carried out using the Improved U-Net Model, which is modified using the optimisation method known as Particle Swarm Optimisation (PSO) algorithm. Improved U-Net Model outperforms such cutting-edge techniques in the plaque segmentation challenge, demonstrating the usefulness and strong explanatory power of the suggested approach.

Keywords: *Medical imaging, Carotid Plaque image segmentation, U-Net Architecture Particle Swarm Optimization (PSO) algorithm and Plaque segmentation.*

How to cite this article: Jonnala P, Reddy GS, An Improvedu-Net Model for Carotid Plaque Segmentation. Int J Drug Deliv Technol. 2026;16(5s): 191-200. DOI: 10.25258/ijddt.16.5s.23

Source of support: Nil.

Conflict of interest: None

1. INTRODUCTION

Modern medical experts are concentrating more on technology methods for treating a range of ailments. The degree of atherosclerotic vascular narrowing has been connected to the natural course of carotid artery disease, and two large randomised studies have demonstrated that preventative carotid endarterectomy in symptomatic individuals with high-grade stenosis provides therapeutic advantages. Recent research has also revealed that surface characteristics and the appearance of the atherosclerotic plaque, as measured by ultrasonography B-mode imaging, are important [1,2], may be of pathogenic significance. In comparison to homogeneous echogenic plaques, heterogeneous and echo lucent plaques, as well as ulcerated plaques, may increase the risk of stroke. B-mode high-resolution ultrasonography is one of the most effective non-invasive methods for detecting atherosclerotic conditions early. High-resolution ultrasonography provides information on atherosclerotic plaque's sizes and consistencies, as well as the degree of carotid artery stenosis and other arterial wall properties.

Following the progression of atherosclerotic disease can be made easier for medical professionals as for identifying plaqued areas in ultrasonic B-mode images using segmentations [29] of carotid arteries. To assess susceptibility to plaques, elasticity maps produced from ROI (regions of interest) of arterial walls in a few cardiac cycles. Consequently, it is advantageous to segment ROIs using series of ultrasound (US) images. Algorithmic segmentations with minimum user engagements are essential in research contexts because of the time needed to manually execute segmentation tasks and variability of intra/inter-observers.

There have been several documented methods for segmenting carotid arteries with plaque using US imaging. Using longitudinal 2D images of carotid plaques and initializations based on blood flow images, many snake segmentations were attempted. Segmentations based on based on pixel intensity using gradients, snake shapes, semantics, and fuzzy K-means have identified plaques in 2D longitudinal images. Longitudinal 2D and cross sectional images of plaques were segmented using Hough transformations.

The creation of novel image segmentation models with improved performance and high accuracy rates on many well-known datasets has been aided in recent years by DL networks [5]. Image segmentations can be based on semantics or instances. Semantic segmentations may be viewed as classification issues for pixels where pixels are assigned to certain classes using segmentations of interesting objects in input images were identified via instance segmentations. In order to provide an effective and flawless plaque segmentation solution, this study presents a better segmentation method integrating PSO and U-Net segmentation. Numerous studies on segmentations of B-mode images and segmentations of

**Author for Correspondence: jp_ece@vignan.ac.in*

plaques discovered that Improved U-Net Models significantly improve average accuracies of segmentations.

The parts that follow are organised as follows. Section 2 presents a number of research that are connected to the techniques for plaque segmentation in medical images. The structure of the many approaches employed in the suggested method is explained in Section 3. Section 4 contains a detailed overview of the experimental findings. Finally, Section 5 offers a summary and recommendations for next study.

2. RELATED WORKS

A variety of segmentation properties and methods have been carefully examined in a number of articles over many years. Applicable solutions have been found for segmenting variety of interesting objects, significant differences in their properties in images, various medical imaging modalities, and associated changes in signal homogeneities, inconsistencies, and noises for objects. The most common medical image segmentation approaches are outlined in this section along with their capabilities, fundamental benefits, and basic drawbacks.

To automatically differentiate carotid plaques, Li et al [2022] [6] developed FRDDNet, a new DCNN (deep convolution neural networks) using encoders/decoders for enhancing the dependability of obtained features. The study used FRMs (feature remapping modules) and inserted them into encoded/decoded blocks. The encoding of features was executed while a novel dense decoding strategy decoded the components. The study also developed compound loss functions to sharpen networks and increase their resilience.

Zhou et al [2021] [7] trained segmentation model using the suggested modified U-Net, which also produced the TPA measurement. The study employed 510 plaques from 144 patients in total, and the data set was randomly divided as test/training groups of 2/3 and 1/3. Monte Carlo cross-validation was performed. The 510 plaques that served as the ground-truth references were manually delineated by two observers who had received training in doing so. To evaluate the parameters of accuracies, variability, and sensitivities of data, two U-Net models (M1 and M2) were trained on two separate datasets for two observations and strong agreements between two manual segmentations and the algorithmic segmentations achieved Pearson correlation coefficients r = 0.989 (p 0.0001) and r = 0.987 (p 0.0001) in demostrations.

Images of ICAs m (internal carotid arteries) and CCAs (common carotid arteries) were used to identify carotid plaques using a suggested UNet DL model based on channel attentions by Jain et al [2022] [8]. In this study, 970 images of ICAs (UK) and 379 images of diabetic CCAs (Japan), and 300 images CCAs from postmenopausal women in Hong Kong were used. Adding two CCAs together, an integrated database of 679 shots was formed. The experiment's database was tripled when 679 CCAs imagegraphs were added using a rotation correction method. The cross-validation K5 (80% training: 20% testing) approach was employed to measure accuracy.

Guo et al [2021] [9] suggested a method that, after segmenting and measuring the intima-media membrane with SVMs (support vector machines), detects the ROI with CNNs (convolution neural networks). The membrane detection problem is fundamentally a target detection problem. The method employs a revolutionary detection technique known as YOLO (Yon Only Look Once) includes a convolution neural network technique for end-to-end training. With a 95% ground truth consistency rate, the programme accurately and effectively predicts the intima-media thickness in ultrasound images.

A unique approach of RDWTs (rational-dilation wavelet transforms) was presented by Mailerum Perumal et al [2022] [10] for classifying and describing carotid plaque in ultrasound images. RDWTs were mainly employed for enhancing images where pre-processing, feature extraction, and ensemble classifications are automated plaque categorizations. Classifiers for plaque Classifications use PNN (Probabilistic Neural Networks), KNN (K Nearest Neighbour), and SVM. Experiment results show how the proposed approach works in terms of accuracy, specificity, and sensitivity. When compared to current techniques such as KNN, PNN, and SVM, the proposed method achieves 93% accuracy, 90% sensitivity, and 94% specificity.

Golemati and colleagues [2020] [11] used xross-correlations of displacement waveforms to determine synchronisation patterns of various tissue sections. The average phase shift in 135 plaques (77 individuals) was 0.4 seconds, and the plaque's radial distortion and the artery's diameter were 50% synchronised. For echogenicity, symptomatology, degree of stenosis, and plaque risk, respectively, Classifications of phase-shift-based parameters using RFs (Random Forests) produced Area-Under-the-Curve scores of 0.81, 0.79, 0.89, and 0.90.

Latha et al [2021] [12] proposed a completely automated DBSCAN (Density Based Spatial Clustering of Applications with Noise) is used for better and self-learning based segmentations by extracting edges using modified propagation affinities. Variety of performance metrics including GVFs (Gradient Vector Flows), snake models and PSO clustering based segmentations were evaluated segmentations results. The study's proposed parameter free automated segmentation technique, which employed DBSCAN and affinity propagations to provide conclusions supported by longitudinal B-mode ultrasound images, was evaluated using a database of 361 images. The suggested method improves segmentation accuracy by 12% when compared to manual segmentation and by 15% when compared to segmentation using affinity propagation and DBSCAN when done separately.

de Ruijter et al [2020] [13] created a pipeline for automatic segmentation. The size and approximate centre of the vessels for each frame were first determined using

the Star-Kalman technique. Before being converted into 2D monogenic signals, Gaussian high pass filters cleaned the images. The lateral wall-lumen contrasts were enhanced using these data to restore multi-scale asymmetric characteristics. These images and their original elliptical outlines along with their active deformable contour models, segmented vascular lumens. The lumen-plaque borders were segmented using Otsu thresholds. A filtering approach was utilised to lessen distension of walls brought on shifts in blood pressures. Finally, patient specific solid mechanic models of whole artery walls were constructed using contours as 3D hexahedral meshes. The common carotid arteries had an average Hausdorff distances of 0.86 mm and similarity indices of 0.91, according to the study.

Jain et al [2021] [14] to segment the atherosclerotic wall with the least amount of plaque, a four-layered UNet design was adopted. Studies utilising both visible and invisible AI have been conducted. For evaluations, wall plaque areas were measured. Subsequently, statistics confirmed dependability and stability of the proposed technique. The Unseen AI pair's mean accuracy, dice-similarity, and correlation coefficient were 98.55, 78.38, and 0.80 (p 0.0001) while utilising the suggested UNet DL architectures.

3. PROPOSED METHODOLOGY

In this study, an improved U-Net model is suggested for segmentation with more precise and understandable sematic segmentation of medical images, as illustrated in Fig. 1. The method of enabling any neural network to have sequence information in both forward and backward directions is known as the suggested classifier. The counts of weights and hidden neurons in the network is decreased by computing the suggested enhanced U Net classifier, weight, and bias values in a cell using PSO. The success of the suggested strategy is demonstrated by the fact that the upgraded U-Net classifier performs the task with noticeably greater accuracy than those state-of-the-art approaches. Metrics.

3.1. Dataset Description:

694 volunteers' CCA images are available in the database. This research, which complied with the Declaration of Helsinki, examined 1,088 people. 2176 total CCA ultrasonography images were obtained from the neck's left and right sides. The imagegraphs were taken between 2003 and 2007 in the Cyprus villages of Pedoulas, Nissou, and Kambos (694 participants, 1388 imagegraphs). The population list was used to identify every resident of the three villages in Cyprus, and those over 40 were asked to take part. Up to 2017 (mean follow-up: 11 3 years), the Cyprus participants were monitored, and any subsequent cardiovascular events or fatalities were recorded. Philips (ATL) HDI 5000 duplex scanner (Seattle, WA, USA) with a broadband L12-5 MHz linear array transducer was used for all scans from Cyprus.

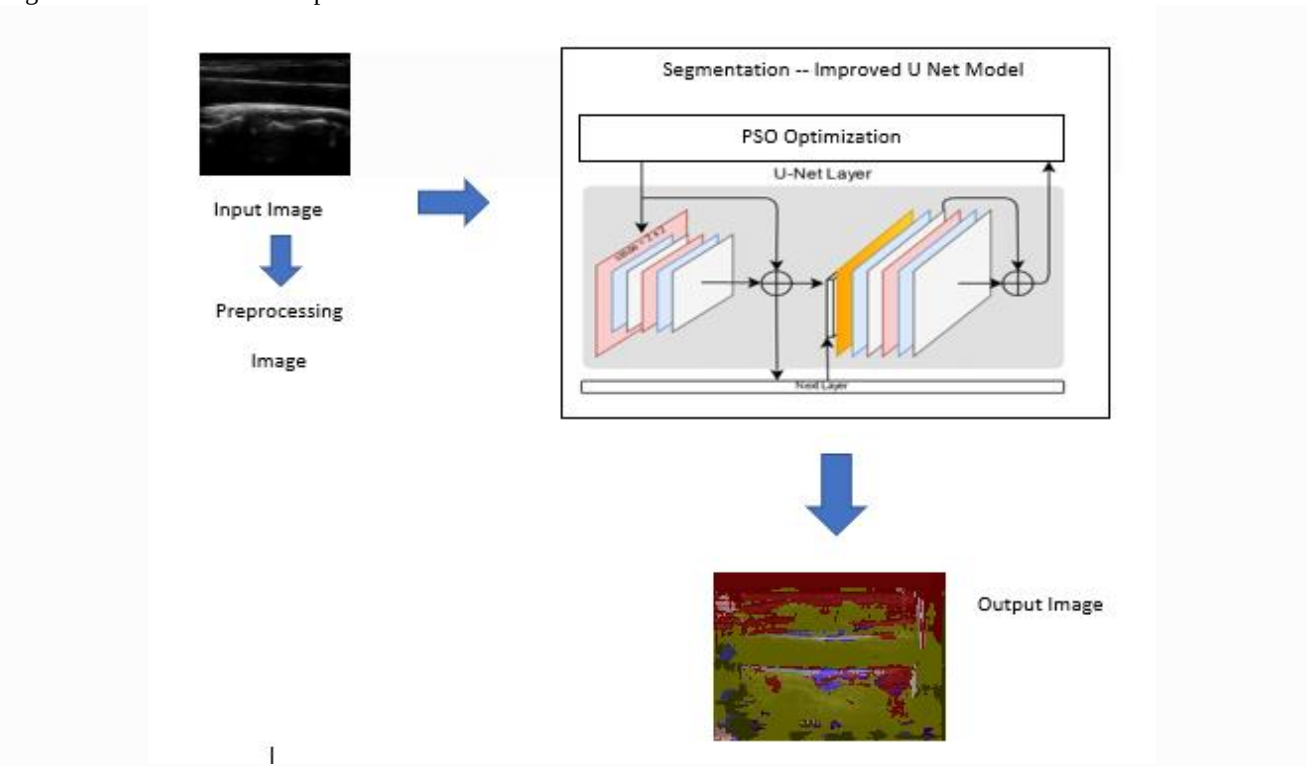

Fig.1. Improved U Net Model for Plaque segmentation

3.2. Pre-Processing:

The most important work in medical imaging is pre-processing since it identifies aberrant parts that cannot be seen by visualising the image but can be seen by CAD systems. Here, processing the image makes use of the image resize idea [17,18]. To change the total counts of pixels in the image, image resizing is required. The

imagegraph was captured in [224 224] format. The pre-processed image's output is given to the following phase.

3.3. Segementation using Improved U-Net Model

Segmenting US images may be difficult to discern because to low contrast in certain plaque sites, shadowed from calcified plaques, and irregular morphologies of other plaques. The CCA plaque, however, appears black and homogeneous in US images [19,20] the substitution of supervised learning-based supervised semantic segmentation (SS) methods for pixel- or shape-based image characteristics. They use an inference, learning process to turn any size of image as input data in segmented images with same spatial resolutions. In this case, segmentations into plaque segmentation jobs with the objective of classifying pixels into two groups: pixel of plaque and outside plaque regions.

Prior to normalising the images to a size of 128 X 128 pixels, the sematic segmentation of the images was first acquired in accordance with the segmented data. A modified version of U-Nets demonstrated great performances in medical image segmentations [21,22], was used to segment the plaque. U-Nets provides complete automated segmentation solutions, with encoder networks extracting features from input images, corresponding decoder networks reconstructing feature maps similar to original image sizes, and soft-max layesr categorising feature map picxels into plaque and non-plaque regions. As shown in Fig. 2, the convolution network design for the encoder part (left side) consists of four blocks. Each block consists of a drop-out layer, two repeated 3 X 3 convolutions, a rectified linear unit (ReLU), and a 2 X 2 max-pooling operation with a stride of 2. To prevent the network from overfitting, the dropout layer randomly sets input elements to zero at a predetermined frequency.

In the decoder portions (right side), an up-sampling block is made up of two 2 X 2 up-convolutions, concatenations with the same feature masp from coded areas, two 3 X 3 convolutions, and ReLU. A 1 X 1 convolution layer is then used as the last layer to convert each 64-component feature vector to a 2D vector. Then, each pixel is divided into two groups: those that are inside the plaque and those that are outside the plaque using a pixel-by-pixel soft-max layer. The result of the pixel-wise soft-max layer is as follows: Assuming that channel i was applied at location (x, y) to monitor neuron activity, ai x; y,

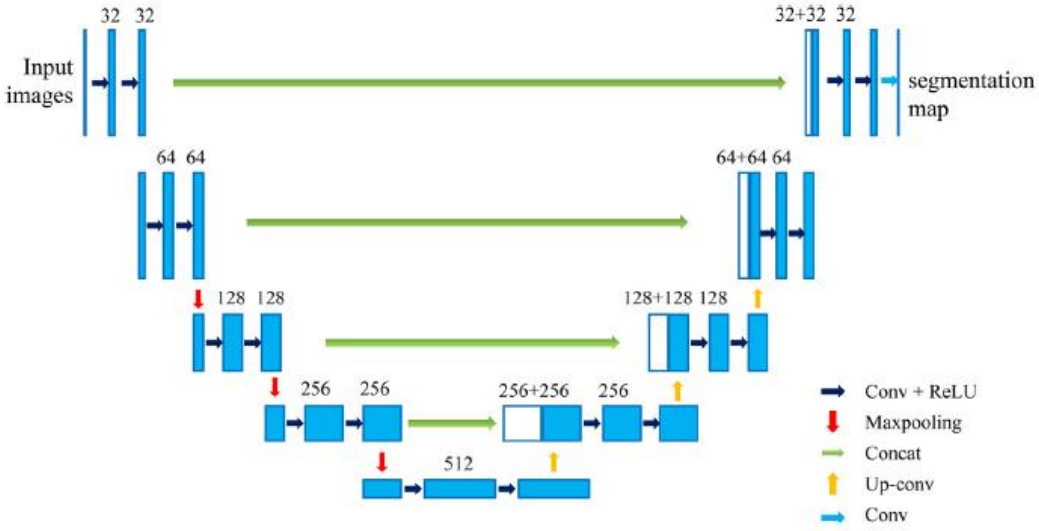

Fig. 2. Architecture of U-Net

$$p^i(x,y) = \frac{\exp(a^i_{x,y})}{\sum_{j=1}^{K} \exp(a^j_{x,y})} \quad \textbf{(1)}$$

K represents courses and cross-entropies loss functions compute energy functions. The plaque serves as the foreground in our application, whereas the area outside the plaque serves as the backdrop [23,24]. Suppose the backdrop is labelled 0, and the plaque region is labelled 1. The output of the soft-max layer's divergence from 1 is then penalised by the cross entropy using:

$$w(x,y) = \frac{1}{N}\sum_{i}^{N} mask_i(x,y) \quad \textbf{(2)}$$

Mask (x, y) are labels in training images at positions (x, y), where plaque pixels in mask images are labelled as 1 and background pixels as 0, N stands for counts of training

images, i implies image indices, and mask (x, y) represents labels in training images at location (x, y).

A neural network's learning performance may be improved by effectively classifying or predicting data from several test sets after it has been trained with a single data set to generate the closest approximation of generalised answers. Choosing the best learning rate is crucial because it affects whether or not the network converges to the global minima. There is a very good possibility of overshooting the global minima when using a high learning rate and global minimum, but they never approach it. A neural network can converge to the global minima by choosing a low learning rate, but it takes a very long time. hence, to give the network more training time. Additionally, the network is more likely to become trapped in a local minimum when learning rates are low. i.e., because of the low learning rate, the network will converge on a local minimum and be unable to escape it. As a result, the first hidden layer's nodes are picked adaptively based on PSO in order to choose the learning and increase prediction accuracy. This enhances the network's dynamic learning rate and quick convergence.

PSO searches for the optimal answer using a counts of particles [25] that move around as a swarm in the search space. Particles are as points in a D-dimensional spaces that change their “flights" in accordance theirs and other particles' prior flying experiences [31]. To locate the ideal solution, the particles move across the D-dimensional space at a specific speed.

Velocities of particles i can be expressed as $V_i = (v_{i1}, v_{i2}, \ldots, v_{iD})$, with locations $(x, x_{i2}, \ldots, x_{iD})$,, and optimal locations expressed as$p_g = (p_{g1}, p_{g2}, \ldots, p_{gD})$, it is also called p_{best}.

Global optima position of particles (g_{best})can be expressed ss $p_g = (p_{g1}, p_{g2}, \ldots, p_{gD})$, Particles in groups have fitness functions to compute fitness values. In standard PSOs, velocity update formulae of the dimension’s d can be related to equations (20) and (21):

$$v_{id} = w \times v_{id} + c_1 \times rand() \times (p_{id} - x_{id}) + c_2 \times Rand() \times (p_{gd} - x_{id}) \quad \textbf{(3)}$$

$$(X_{id} = x_{id} + v_{id}) \quad \textbf{(4)}$$

The following parameters are part of the PSO: Q (Population Quantity), w (inertia weight), C1 and C2 (acceleration constants), vmax (the maximum velocity), Gmax (the maximum counts of repetitions), rand () and Rand (), which are random functions with values between 0 and 1. C1 and C2 are typically valued using constant 2.

The PSO overcomes the constraints of traditional optimisation methods in handling multiparameter, strong coupling, and nonlinear engineering optimisation problems by improving information transfer across populations and maintaining population variety. These restrictions include the potential to readily slip into local optimisation and advanced convergence [26,27]. The phrase "local-global information sharing" that was imported has its parameters examined, and the selection of parameters for performance is established. The effectiveness of the PSO's global search is then validated by comparing its performance to that of several sets of traditional optimisation techniques.

The objective of this study is to present a PSO version that seeks to enhance U Net's effectiveness in locating superior solutions while maintaining both its simplicity and rapid convergence. Figure 3 shows the suggested model.

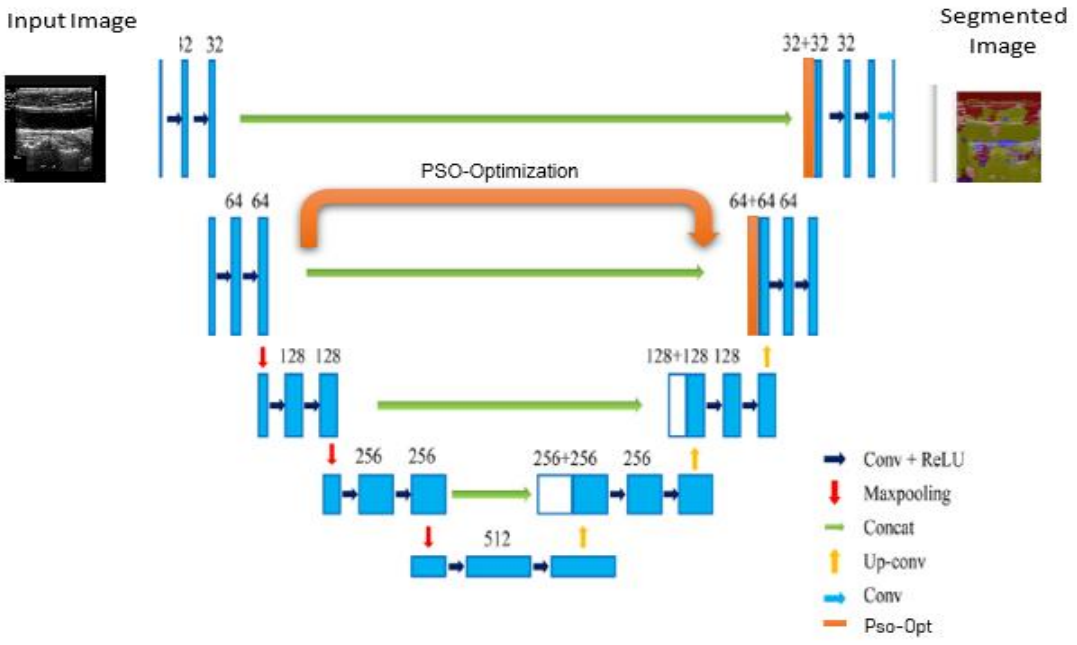

Fig. 3. Architecture of Proposed Model

The Proposed U-Net segmentation task as follows:

1. **Network architecture:** U-Net architectures were streamlined from five to four convolution blocks, and counts of fundamental convolution kernels were decreased from 64 to 32 because the size of input images for CCAs were 128 by 128 pixels, which were smaller than size of input images in original UNets [28, 30].
2. **Dropout:** After convolution blocks of encoders, drop-out hidden layers were added that randomly sets input elements to zero with probabilities of 50%, preventing overfitting in planned U-Nets.
3. **Hyper parameters of PSO:** This is a learning algorithm with a variable learning rate. The approach employs first- and second-order moment estimations to dynamically adjust parameters and learning rate, which can greatly accelerate optimisation convergence.
4. **Cross-entropy loss function with weight map added:** The class frequencies in the training data set were taken into account while adding a weight map to the loss function.

4. EXPERIMENTAL RESULTS AND DISCUSSION

Recent studies have demonstrated that, in comparison to employing a single modality, the discriminative performance tends to be better by taking into account all of the characteristics from several modalities. Because these two give rich and varied intensities within the data, radiomic approaches based on the Improved U Net model were therefore proposed in the current study. Table 1 shows the segmentation output and sample input image.

Table 1. Sample Output of Proposed Work

Input Image	Binary Image	Segmentation Image
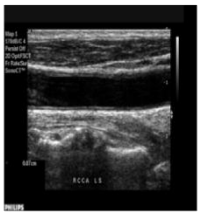	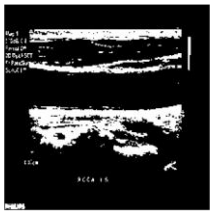	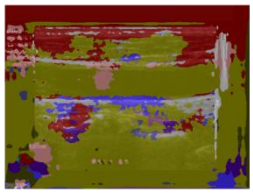
	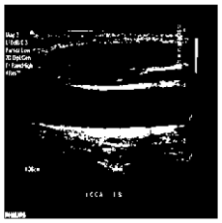	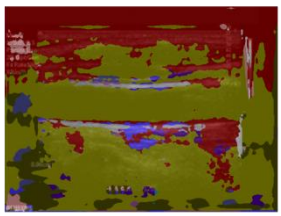
	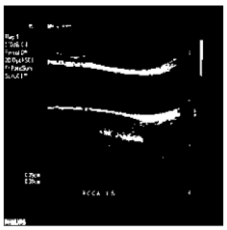	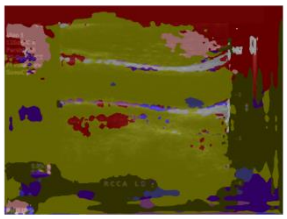

This work computed the confusion matrix, which summed a classifier's segmentation performance on the test dataset. DSC (F1-score), accuracy, IOU, and comparison with existing approaches such as U-Net, Dilated U-Net, and Improved U-Net. In this scenario, the parameter (DSC) is used to compute the precise amount of ratio of the available actual or plaque and available plague or non-plague pixels to the expected pixels, and it is computed using the following equation: The F1-score is defined as follows:

$$F1 - score = \frac{2 \times precision \times recall}{precision + recall} \quad \textbf{(5)}$$

The first is a non-plaque mass classed as Non-Plaque (True Negative), followed by a Non-Plaque mass classified as Plaque (False Positive), a Plaque mass classified as Plaque (TP), and lastly a Plaque mass classified as Non-Plaque (FN). These four measures are the primary components of the confusion matrix, which is one of the key metrics used to assess segmentation accuracy. True Negative (TN) and True Positive (TP) values were also measured and used to determine the following:

$$Pixelaccuracy = \frac{TP + TN}{TP + FN + TN + FP} \quad \textbf{(6)}$$

IOU: is a metric for calculating the precision of identifying plaque in imagegraphs. The Intersection Over Union (IOU) measure was used to assess how accurate the model is in localising plaque in the sample, as follows:

$$IOU = \frac{AO}{AU} \quad \textbf{(7)}$$

Where AO stands for Area of Overlap and AU stands for Area of Union. In this study, the mass is considered properly identified if IOU values are greater than equal to 0.5; else, the detection is ignored. The results of performance comparisons are provided in Table.2.

Table.2. Performance comparison results

Metrics	Methods		
	U-Net	**DU-Net**	**IMU-Net**
Pixel Accuracy	80	80.12	94.611
F-measure	78	86.45	91.09
IOU	68	70.00	94

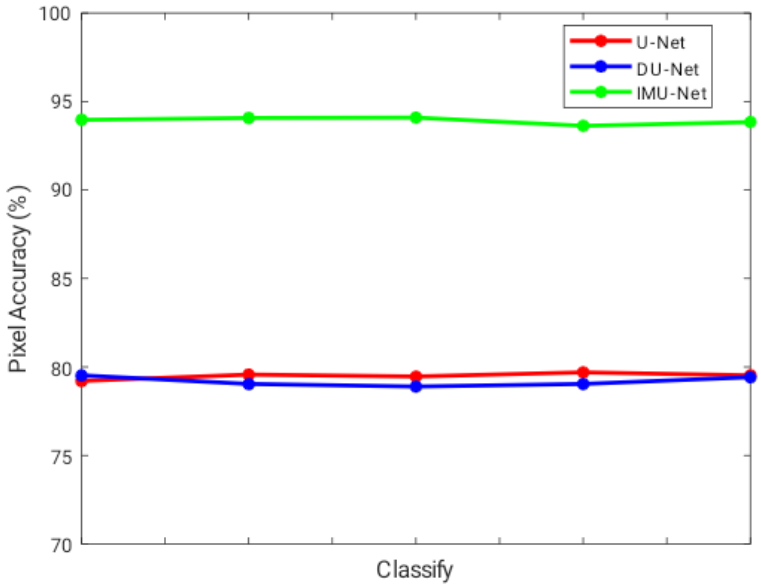

Fig.4. Pixel Accuracy comparison results between the proposed and existing method for segmentation of the Carotid Plaque data

Figure 4 shows the pixel accuracy comparisons between the suggested and existing methods for segmenting Carotid Plaque data. The findings show that the suggested Improved U Net Model approach outperforms existing segmentation algorithms in terms of pixel accuracy.

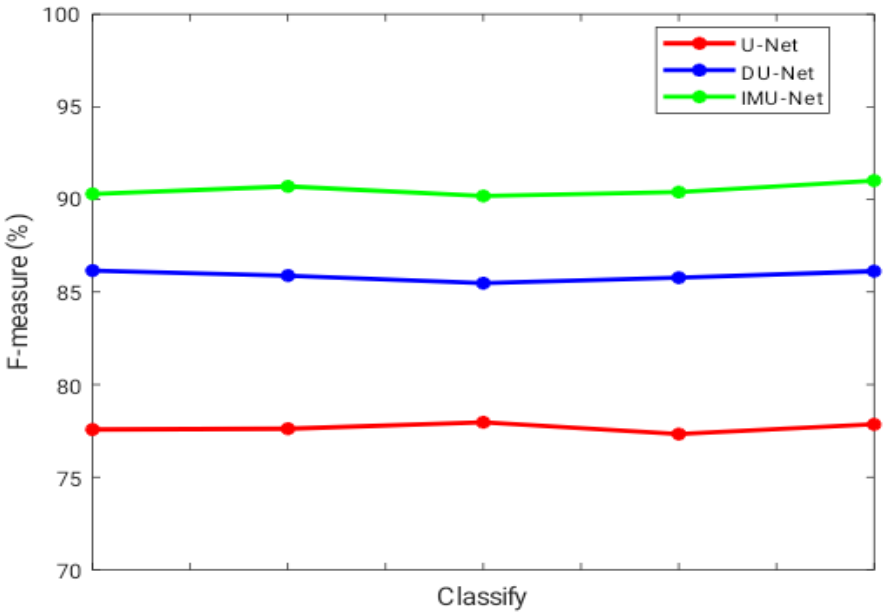

Fig.5. F Measure comparison results between the proposed and existing method for segmentation of the Carotid Plaque data

Figure 5 shows the f measure comparisons between suggested and existing methods for segmenting Carotid Plaque data. The findings show that the proposed Improved U Net Model approach outperforms existing segmentation strategies in terms of f measures.

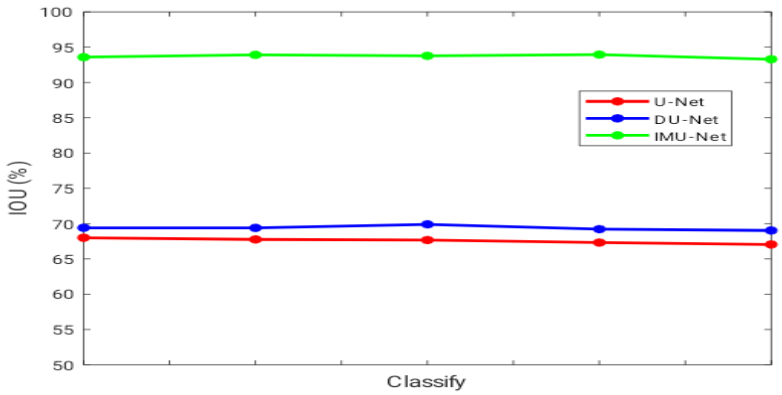

Fig.6. IOU comparison results between the proposed and existing method for segmentation of the Carotid Plaque data

Figure 6 shows the IOU comparative results for the suggested and existing methods for segmenting Carotid Plaque data. The findings show that the proposed Improved U Net Model approach outperforms existing segmentation strategies in terms of IOU.

5. CONCLUSION AND FUTURE WORK

The newest field of study was automated illness diagnosis using medical images based on DL. In the current study, we had highlighted the advantages and shortcomings of the most prevalent DL-based models used for segmentation of medical images. The image segmentation and optimisation steps are crucial in the process of building a model. Plaque that has the least impact can be removed with its aid. Each of the recommended enhanced U Net model solutions for this crucial objective accomplishes good optimisation to a noteworthy degree and provides a novel approach to handling medical data. This technique has been utilised to achieve precision that is almost perfect at every level of life. The proposed initiative will improve categorisation. Finally, the precision, F-measure, and pixel accuracy of Improved U-Net performance are compared to U-Net and dilated U-Net. The enhanced U-Net network topology has been in use and updated for many years as a medical segmentation implementation standard. The concerns outlined in Section 2 have started to be resolved thanks to the effort and advancements made by U-Net in recent years, although certain still remain. This section will highlight some promising research that addresses those issues (accuracy concerns) and introduce other difficulties that could still be present. This study used the DL method to decrease error as well. Deep transfer learning with classification will be used in the future to learn from many datasets.

REFERENCES

1. Fedak, A., Ciuk, K. and Urbanik, A., 2020. Ultrasonography of vulnerable atherosclerotic plaque in the carotid arteries: B-mode imaging. Journal of ultrasonography, 20(81), pp.135-145.
2. Jamthikar, A.D., Gupta, D., Puvvula, A., Johri, A.M., Khanna, N.N., Saba, L., Mavrogeni, S., Laird, J.R., Pareek, G., Miner, M. and Sfikakis, P.P., 2020. Cardiovascular risk assessment in patients with rheumatoid arthritis using carotid ultrasound B-mode imaging. Rheumatology international, 40(12), pp.1921-1939.
3. Jain, P.K., Sharma, N., Giannopoulos, A.A., Saba, L., Nicolaides, A. and Suri, J.S., 2021. Hybrid deep learning segmentation models for atherosclerotic plaque in internal carotid artery B-mode ultrasound. Computers in Biology and Medicine, 136, p.104721.
4. Jamthikar, A., Gupta, D., Johri, A.M., Mantella, L.E., Saba, L. and Suri, J.S., 2022. A machine learning framework for risk prediction of multi-label cardiovascular events based on focused carotid plaque B-Mode ultrasound: A Canadian study. Computers in Biology and Medicine, 140, p.105102.
5. Jain, P.K., Gupta, S., Bhavsar, A., Nigam, A. and Sharma, N., 2020. Localization of common carotid artery transverse section in B-mode ultrasound images using faster RCNN: a deep learning approach. Medical & Biological Engineering & Computing, 58, pp.471-482.
6. Li, Y., Zou, L., Xiong, L., Yu, F., Jiang, H., Fan, C., Cheng, M. and Li, Q., 2022. FRDD-Net: automated carotid plaque ultrasound images segmentation using feature remapping and dense decoding. Sensors, 22(3), p.887.
7. Zhou, R., Azarpazhooh, M.R., Spence, J.D., Hashemi, S., Ma, W., Cheng, X., Gan, H., Ding, M. and Fenster, A., 2021. Deep learning-based carotid plaque segmentation from B-mode ultrasound images. Ultrasound in Medicine & Biology, 47(9), pp.2723-2733.
8. Jain, P.K., Dubey, A., Saba, L., Khanna, N.N., Laird, J.R., Nicolaides, A., Fouda, M.M., Suri, J.S. and Sharma, N., 2022. Attention-based UNet Deep Learning model for Plaque segmentation in carotid ultrasound for stroke risk stratification: An artificial Intelligence paradigm. Journal of Cardiovascular Development and Disease, 9(10), p.326.
9. Guo, D., Zhang, G., Peng, H., Yuan, J., Paul, P., Fu, K. and Zhu, M., 2021. Segmentation and measurements of carotid intima-media thickness in ultrasound images using the improved convolutional neural network and support vector machine. Journal of Medical Imaging and Health Informatics, 11(1), pp.15-24.
10. Mailerum Perumal, A., Balaji, G.N., Dhiviya Rose, J., Kulkarni, A. and Shajin, F.H., 2022. Automated technique for carotid plaque characterisation and classification using RDWT in ultrasound images. Computer Methods in Biomechanics and Biomedical Engineering: Imaging & Visualization, 10(2), pp.187-199.
11. Golemati, S., Patelaki, E., Gastounioti, A., Andreadis, I., Liapis, C.D. and Nikita, K.S., 2020. Motion synchronisation patterns of the carotid atheromatous plaque from B-mode ultrasound. Scientific reports, 10(1), pp.1-13.
12. Latha, S., Samiappan, D., Muthu, P. and Kumar, R., 2021. Fully automated integrated segmentation of carotid artery ultrasound images using DBSCAN and affinity propagation. Journal of Medical and Biological Engineering, 41, pp.260-271.
13. de Ruijter, J., van Sambeek, M., van de Vosse, F. and Lopata, R., 2020. Automated 3D geometry segmentation of the healthy and diseased carotid artery in free-hand, probe tracked ultrasound images. Medical Physics, 47(3), pp.1034-1047.
14. Jain, P.K., Sharma, N., Saba, L., Paraskevas, K.I., Kalra, M.K., Johri, A., Laird, J.R., Nicolaides, A.N.

and Suri, J.S., 2021. Unseen artificial intelligence—Deep learning paradigm for segmentation of low atherosclerotic plaque in carotid ultrasound: A multicenter cardiovascular study. Diagnostics, 11(12), p.2257.

15. Hassanin, D., Khalaf, A. and Gharrieb, R.R., 2021. Automatic localization of Common Carotid Artery in ultrasound images using Deep Learning. Journal of Advanced Engineering Trends, 40(2), pp.127-135.
16. Kostelansky, M., Rodriguez, A.M., Kybic, J., Hekrdla, M., Dvorsky, O., Kozel, J., Baurova, P., Pakizer, D. and Skoloudik, D., 2021, December. Differentiating between stable and progressive carotid atherosclerotic plaques from in-vivo ultrasound images using texture descriptors. In 17th International Symposium on Medical Information Processing and Analysis (Vol. 12088, pp. 511-520). SPIE.
17. de Ruijter, J., van Sambeek, M., van de Vosse, F. and Lopata, R., 2020. Automated 3D geometry segmentation of the healthy and diseased carotid artery in free-hand, probe tracked ultrasound images. Medical Physics, 47(3), pp.1034-1047.
18. Qian, C., Su, E. and Yang, X., 2020. Segmentation of the common carotid intima-media complex in ultrasound images using 2-D continuous max-flow and stacked sparse auto-encoder. Ultrasound in Medicine & Biology, 46(11), pp.3104-3124.
19. Zhou, R., Guo, F., Azarpazhooh, M.R., Hashemi, S., Cheng, X., Spence, J.D., Ding, M. and Fenster, A., 2021. Deep learning-based measurement of total plaque area in B-mode ultrasound images. IEEE Journal of Biomedical and Health Informatics, 25(8), pp.2967-2977.
20. Meshram, N.H., Mitchell, C.C., Wilbrand, S., Dempsey, R.J. and Varghese, T., 2020. Deep learning for carotid plaque segmentation using a dilated U-Net architecture. Ultrasonic imaging, 42(4-5), pp.221-230.
21. Meiburger, K.M., Marzola, F., Zahnd, G., Faita, F., Loizou, C.P., Lainé, N., Carvalho, C., Steinman, D.A., Gibello, L., Bruno, R.M. and Clarenbach, R., 2022. Carotid Ultrasound Boundary Study (CUBS): Technical considerations on an open multi-center analysis of computerized measurement systems for intima-media thickness measurement on common carotid artery longitudinal B-mode ultrasound scans. Computers in Biology and Medicine, 144, p.105333.
22. Jain, P.K., Dubey, A., Saba, L., Khanna, N.N., Laird, J.R., Nicolaides, A., Fouda, M.M., Suri, J.S. and Sharma, N., 2022. Attention-based UNet Deep Learning model for Plaque segmentation in carotid ultrasound for stroke risk stratification: An artificial Intelligence paradigm. Journal of Cardiovascular Development and Disease, 9(10), p.326.
23. Shen, D., Huang, X., Huang, Y., Zhou, D. and Ye, S., 2022. Computed Tomography Angiography and B-Mode Ultrasonography under Artificial Intelligence Plaque Segmentation Algorithm in the Perforator Localization for Preparation of Free Anterolateral Femoral Flap. Contrast Media & Molecular Imaging, 2022.
24. Liapi, G.D., Kyriacou, E., Loizou, C.P., Panayides, A.S., Pattichis, C.S. and Nicolaides, A.N., 2022, June. Deep Learning-Based Segmentation of the Atherosclerotic Carotid Plaque in Ultrasonic Images. In Artificial Intelligence Applications and Innovations. AIAI 2022 IFIP WG 12.5 International Workshops: MHDW 2022, 5G-PINE 2022, AIBMG 2022, ML@ HC 2022, and AIBEI 2022, Hersonissos, Crete, Greece, June 17–20, 2022, Proceedings (pp. 187-198). Cham: Springer International Publishing.
25. Jain, M., Saihjpal, V., Singh, N. and Singh, S.B., 2022. An Overview of Variants and Advancements of PSO Algorithm. Applied Sciences, 12(17), p.8392.
26. Tharwat, A. and Schenck, W., 2021. A conceptual and practical comparison of PSO-style optimization algorithms. Expert Systems with Applications, 167, p.114430.
27. Zhu, Y., Li, G., Wang, R., Tang, S., Su, H. and Cao, K., 2021. Intelligent fault diagnosis of hydraulic piston pump combining improved LeNet-5 and PSO hyperparameter optimization. Applied Acoustics, 183, p.108336.
28. Deng, C., Adu, J., Xie, S., Li, Z., Meng, Q., Zhang, Q., Yin, L. and Peng, B., 2022. Automatic segmentation of ultrasound images of carotid atherosclerotic plaque based on Dense-UNet. Technology and Health Care, (Preprint), pp.1-15.
29. P. Jonnala and G. S. Reddy, "Image de-noising of Ultrasound Carotid artery images using various filters," 2023 4th International Conference for Emerging Technology (INCET), Belgaum, India, 2023, pp. 1-4, doi: 10.1109/INCET57972.2023.10170198.
30. Kothala, L. P., Jonnala, P., & Guntur, S. R. (2023). Localization of mixed intracranial hemorrhages by using a ghost convolution-based YOLO network. Biomedical Signal Processing and Control, 80, 104378.